Evaluation of Neurodegenerative Disorders with Amyloid-β, Tau, and Dopaminergic PET Imaging: Interpretation Pitfalls

Brian J. Burkett, Derek R. Johnson, and Val J. Lowe

Department of Radiology, Mayo Clinic, Rochester, Minnesota

Learning Objectives: On successful completion of this activity, participants should be able to (1) understand the principles of visually interpreting amyloid, tau, and dopaminergic PET scans; (2) understand the role of amyloid, tau, and dopaminergic PET scans in clinical context; and (3) recognize potential pitfalls that could arise in correct visual interpretation and in imaging protocols for amyloid, tau, and dopaminergic PET scans.

Financial Disclosure: Dr. Burkett receives research support from GE Healthcare and the Radiological Society of North America. Dr. Johnson is a consultant for Telix and Novartis. Dr. Lowe serves as a consultant for Bayer Schering Pharma, Piramal Life Sciences, Life Molecular Imaging, Eisai Inc., AVID Radiopharmaceuticals, Eli Lilly and Co., and Merck Research and receives research support from Siemens Molecular Imaging, AVID Radiopharmaceuticals, and the National Institutes of Health (National Institute on Aging, National Cancer Institute). The authors of this article have indicated no other relevant relationships that could be perceived as a real or apparent conflict of interest.

CME Credit: SNMMI is accredited by the Accreditation Council for Continuing Medical Education (ACCME) to sponsor continuing education for physicians. SNMMI designates each *JNM* continuing education article for a maximum of 2.0 AMA PRA Category 1 Credits. Physicians should claim only credit commensurate with the extent of their participation in the activity. For CE credit, SAM, and other credit types, participants can access this activity through the SNMMI website (http://www.snmmilearningcenter.org) through June 2027.

Antiamyloid therapies for Alzheimer disease recently entered clinical practice, making imaging biomarkers for Alzheimer disease even more relevant to guiding patient management. Amyloid and tau PET are valuable tools that can provide objective evidence of Alzheimer pathophysiology in living patients and will increasingly be used to complement ^{18}F-FDG PET in the diagnostic evaluation of cognitive impairment and dementia. Parkinsonian syndromes, also common causes of dementia, can likewise be evaluated with a PET imaging biomarker, ^{18}F-DOPA, allowing in vivo assessment of the presynaptic dopaminergic neurons. Understanding the role of these PET biomarkers will help the nuclear medicine physician contribute to the appropriate diagnosis and management of patients with cognitive impairment and dementia. To successfully evaluate brain PET examinations for neurodegenerative diseases, knowledge of the necessary protocol details for obtaining a reliable imaging study, inherent limitations for each PET radiopharmaceutical, and pitfalls in image interpretation is critical. This review will focus on underlying concepts for interpreting PET examinations, important procedural details, and guidance for avoiding potential interpretive pitfalls for amyloid, tau, and dopaminergic PET examinations.

Key Words: dementia; neurodegenerative; amyloid; tau; brain PET

J Nucl Med 2024; 65:829–837
DOI: 10.2967/jnumed.123.266463

Over 55 million people worldwide live with dementia. The World Health Organization ranks dementia as the seventh leading cause of death (*1*). The most common type of dementia is Alzheimer disease (AD), characterized by neuropathologic hallmarks of extracellular amyloid-β plaques and intracellular hyperphosphorylated tau neurofibrillary tangles (*2*). Aside from AD, many other causes of dementia occur, with distinct neuropathologic features, presentations, and prognoses. Neurodegeneration is a feature of all types of dementia, whereas the underlying neuropathologic mechanism and distribution differ among types (*3,4*). For example, Parkinson disease and dementia with Lewy bodies are characterized by pathologic α-synuclein deposition, and pathologic tau deposition can underlie corticobasal degeneration and progressive supranuclear palsy (*5*).

Neuropathologic changes in dementia precede clinical onset during a latent period in which lab and imaging studies such as PET can detect abnormalities. Between different types of neurodegenerative entities, variations and overlap in clinical presentation and neuropathologic changes can lead to diagnostic ambiguity (*3*). For this reason, multiple imaging biomarkers for neuropathologic changes are useful for evaluating dementia in vivo. Furthermore, copathology is common, more so as patients age, which can further complicate and confound accurate diagnosis. With the clinical availability of targeted amyloid therapies for AD and other amyloid- and tau-targeted therapeutic agents under investigation, parsing out an accurate neurodegenerative diagnosis based on imaging biomarkers is more germane to clinical practice than ever before (*6,7*). The inaccurate characterization of a patient's underlying neurodegenerative disease may lead to inappropriate therapy, suboptimal supportive care, and provision of incorrect prognostic information. Nuclear medicine studies using multiple PET radiotracers assess an array of biomarkers that can be useful in the diagnosis and differentiation of neurodegenerative processes. This educational article will discuss the role of PET imaging of multiple imaging biomarkers in the evaluation of dementia, specifically amyloid, tau, and dopaminergic PET.

For AD, a conceptual framework, the ATN classification, has been introduced that incorporates categories of biomarkers for neuropathologic changes into a sequential model, reflecting the hypothesis that amyloid-β plaques ("A") develop initially, followed by pathologic tau deposition ("T"), neurodegeneration ("N"), and finally memory impairment and functional decline. Relevant biomarkers for measuring features of AD pathophysiology in living patients can be classified into one of these categories

Received Nov. 8, 2023; revision accepted Apr. 3, 2024.
For correspondence or reprints, contact Brian J. Burkett (burkett.brian@mayo.edu).
Published online Apr. 25, 2024.

TABLE 1
ATN Biomarker Framework

ATN category	Pathophysiology	Biomarker(s)
A	Amyloid-β proteinopathy	Amyloid PET
		CSF hybrid ratios
		Amyloid-β42/40
		p-tau 181/amyloid-β42
		t-tau 231/amyloid-β42
T	Tau proteinopathy	Tau PET
		CSF hybrid ratios:
		Amyloid-β42/40
		p-tau 181/amyloid-β42
		t-tau 231/amyloid-β42
N	Neurodegeneration (injury of neuropil)	^{18}F-FDG PET
		MRI (volume assessment)
		CSF total tau
I	Inflammation (astrocyte activation)	CSF GFAP
V	Vascular brain injury	MRI (infarcts, white matter T2 hyperintensity, and abundant dilated prevascular spaces)
S	α-synuclein	CSF α-synuclein-SAA

CSF = cerebrospinal fluid; p-tau = hyperphosphorylated tau; t-tau = total tau; GFAP = glial fibrillary acidic protein; SAA = seed amplification assay.

(Tables 1 and 2) (*6,8*). Amyloid and tau PET are important imaging biomarkers for this framework. Neurodegeneration includes both decreased metabolic neuronal function as assessed by ^{18}F-FDG PET and structural changes such as volume loss, detected by MRI. The combined grouping of MRI and ^{18}F-FDG PET data into the neurodegeneration category is a limitation of the framework, as abnormalities on ^{18}F-FDG PET can precede structural changes on MRI, predict progression of cognitive decline, and categorize types of neurodegenerative conditions in the absence of specific changes on MRI (*9,10*). Although the ATN classification is a research framework and not intended as a clinical diagnostic staging mechanism for AD, it is useful to understand that PET examinations represent an array of biomarkers that underlie the biologic features of AD and illustrate that variable results in markers for tau and neurodegeneration can be seen in the Alzheimer continuum (Table 2) (*6*). This framework is actively being updated by the Alzheimer Association workgroup to incorporate additional biomarkers, including biomarkers for comorbid pathology such as vascular injury, neuroinflammation, and α-synucleinopathy. Further details of the revised criteria can be reviewed in a working draft currently available (Tables 1 and 2) (*6,11*). In clinical practice, ^{18}F-FDG PET and amyloid PET have complementary roles in that ^{18}F-FDG PET patterns can suggest alternative neurodegenerative diagnoses. Characteristic regions of AD pathology may be abnormal on ^{18}F-FDG PET in alternative non-AD causes of dementia and cognitive impairment, in which case amyloid PET may help clarify the diagnosis. The role of ^{18}F-FDG PET and MRI in dementia is discussed more extensively in other articles focused on those modalities (*4,12*). In addition to PET, serum and cerebrospinal fluid biomarkers for neuropathologic amyloid-β and tau can also be used but have the disadvantage of lacking information about spatial distribution. Corresponding to the spatial distribution of neurodegeneration, Alzheimer pathology can result in varied clinical presentations besides the more typical amnestic cognitive impairment, including

TABLE 2
NIA-AA Diagnostic Framework Classification

Research framework category	ATN classification
Normal	A− T− (N)−
AD pathologic change	
Alzheimer continuum	A+ T− (N)−
AD	A+ T+ (N)−
	A+ T+ (N)+
AD + suspected non-AD pathologic change	A+ T− (N)+
Non-AD pathologic change	A− T+ (N)-
	A− T− (N)+
	A− T+ (N)+

This framework is actively being updated, incorporating biomarkers of inflammation, vascular injury, and evidence of comorbid pathology. Furthermore, distinction will be made among tau PET staging categories of T_{MTL} (positive only in medial temporal lobes), T_{MOD} (moderate uptake in neocortical regions), and T_{HIGH} (high uptake in neocortical regions). For purposes of this article, only core biomarkers with regulatory approval are included. Proposed update can be accessed online (https://aaic.alz.org/diagnostic-criteria.asp#guidelines).

TABLE 3
AD Therapeutics

Drug	Phase 3 clinical trial	Trial finding summary	Current FDA status
Aducanumab	EMERGE, ENGAGE, NCT02477800, NCT02484547	Both halted at 50% enrollment on basis of futility analysis; EMERGE: Over 78 wk, average 22% slowing of cognitive decline in high-dose arm of study	Accelerated approval
Lecanemab	CLARITY-AD, NCT003887455	Over 18 mo, average 25% slowing of cognitive decline	Approved
Donanemab	TRAILBLAZER-ALZ2, NCT04437511	Over 18 mo, average 35% slowing of cognitive decline	Not approved; under consideration

posterior cortical atrophy, limbic predominant AD, behavioral variant/dysexecutive AD, and logopenic primary progressive aphasia. Interpreting multiple imaging biomarkers together and putting the spatial distribution of changes into context can help increase diagnostic certainty when an atypical AD presentation is suspected.

After AD, Parkinson disease is the second most common neurodegenerative condition. In Parkinson disease, intracellular Lewy bodies—aggregates of α-synuclein—drive degeneration of striatal dopaminergic neurons (*13,14*). L-6-^{18}F-fluoro-3,4-dihydroxyphenylalanine (^{18}F-DOPA) is a PET radiopharmaceutical that can detect uptake of dopamine precursor molecules in viable presynaptic dopaminergic neurons. Atypical parkinsonian disorders are also characterized by dopaminergic neurodegeneration but not necessarily Lewy body pathology. ^{18}F-DOPA can be useful for detecting striatal dopaminergic neuron loss in these conditions with high sensitivity and specificity above 90% (*15*).

AMYLOID PET

The guidelines of the Society for Nuclear Medicine and Molecular Imaging and the European Association of Nuclear Medicine define clinically appropriate use of amyloid PET, indicated in the setting of objective evidence of unexplained mild cognitive impairment assessed by a dementia expert. Amyloid PET is also appropriate for those who meet clinical criteria for possible AD but with uncertainty about the diagnosis, as well as patients who have progressive dementia at an atypically early age (<65 y) (*16,17*). Recently, disease-modifying amyloid antibody therapies have entered clinical practice. Confirmation of abnormal amyloid-β deposition as a therapeutic target may be obtained with amyloid PET (Table 3) (*18–21*). The clinical trials leading to accelerated U.S. Food and Drug Administration (FDA) approval of the amyloid-targeted therapies aducanumab and lecanemab used amyloid PET as a method to define amyloid-β positivity, a core inclusion criterion for the trials, as well as to evaluate therapeutic efficacy (*19–21*). Amyloid clearance measured on PET was a trial endpoint for both aducanumab and lecanemab (*19,20*). Follow-up amyloid PET scans after administration of antiamyloid therapies may be clinically useful for assessing response to treatment, in parallel to the use of amyloid PET as a biomarker in trials, although accessibility for this use is limited by reimbursement. For example, decreased amyloid-β deposition as evaluated by PET after lecanemab was correlated with the therapeutic benefit of delayed cognitive decline (*20*). Amyloid PET may provide clinically useful prognostic information when weighing the risks and benefits of continued therapy.

The amyloid radiotracer ^{11}C-Pittsburgh compound B was the first available amyloid tracer and has been used extensively in the research setting (*22*). At present, 3 amyloid radiotracers have FDA approval: ^{18}F-florbetaben, ^{18}F-florbetapir, and ^{18}F-flutemetamol (Table 4). Each of these has specific properties and differences in procedural standards and acceptable interpretation methods, as defined in the FDA package inserts (Table 4) (*23–25*). For each, the final goal in interpretation is a binary decision of positive

TABLE 4
Amyloid and Tau PET Radiotracer Properties

Radiotracer	Administered activity (MBq)	Uptake time (min)	PET scan duration (min)	Display parameters	Link to training modules
Amyloid-β					
^{18}F-florbetaben	300	45–130	20	Grayscale	https://www.neuraceqreadertraining.com/learn
^{18}F-florbetapir	370	30–50	10	Grayscale	https://amyvid.myregistrationp.com/amyvid/index.do
^{18}F-flutemetamol	185	90	20	Color scan (rainbow, vendor-specified)	https://www.readvizamyl.com/
Tau					
^{18}F-flortaucipir	370	80	20	Color scale (2 colors); transition at 1.65× cerebellar average	https://tauvidreadertraining.com/login/signup.php

or negative. As more experience with antiamyloid therapy accumulates, the ability to monitor changes and therapeutic response with amyloid PET may influence patient management decisions. If amyloid PET is used for monitoring treatment response, as has been done in the clinical trial setting, quantification techniques will also likely become germane to clinical interpretation.

For all FDA-approved amyloid tracers, image interpretation should be performed without consideration of collateral clinical information, mirroring the methods used in clinical studies assessing the radiotracers' performance (*4*). Although this approach may be counterintuitive, the aim is not to synthesize comprehensive information into a clinical diagnosis such as AD but rather to categorize the PET as a positive or negative biomarker for amyloid-β in an unbiased manner.

For all amyloid tracers, the underlying principle for image interpretation is that the tracer binds to normal white matter but spares gray matter. In a normal (negative) scan, this results in a clearly visible outline of the branching white matter structures (Fig. 1). Loss of gray–white differentiation, outward extension of radiotracer from the white matter to the cortical surface, or more intense gray matter radiotracer binding relative to white matter are features of abnormal scans.

For ^{18}F-fluorbetapir, a method for systematic image interpretation of grayscale axial images is defined, starting with inspection of the cerebellar gray–white differentiation and proceeding to the occipital lobe, the temporal lobe, the frontal lobe, and finally the parietal lobe. Each of these lobes in both hemispheres count as one region. A total of 2 regions must be abnormal for a scan to qualify as positive on the basis of loss of gray–white differentiation; however, one abnormal region may qualify a scan as positive on the basis of cortical uptake exceeding the adjacent white matter (*24*).

For ^{18}F-florbetaben, a similar method is defined scrolling from inferior to superior but with slightly different regions, starting with the cerebellum and proceeding to the temporal lobe, frontal lobe, precuneus and posterior cingulate, and finally the parietal lobe. These regions may contribute to a positive scan designation, with the precuneus and posterior cingulate considered separately from the parietal lobe. Positive scans require abnormal uptake in most slices within a brain region, and this uptake can be further subdivided into moderate amyloid-β deposition (small areas of abnormal uptake within ≥1 region) or pronounced amyloid-β deposition (large and confluent areas of abnormal uptake within ≥1 region) (*25*).

For ^{18}F-flutemetamol, a manufacturer-specified color scale should be used with the pons set at 90% of the maximum intensity and a minimum intensity of 0. The following regions are reviewed separately in specified planes, each of which counts toward criteria for a positive scan: the frontal lobe (axial, optional sagittal), the precuneus/posterior cingulate (sagittal, optional coronal), the lateral temporal lobe (axial, optional coronal), the inferolateral parietal lobe (coronal, optional axial), and the striatum (axial, optional sagittal) (*23*). The striatum is assessed only for ^{18}F-flutemetamol, and the optional sagittal plane can be helpful for detecting a normal striatal gap between the frontal white matter and the thalamus.

Regionally positive amyloid PET scans can be more difficult to identify, and it is necessary to scrutinize each lobe of the cerebral

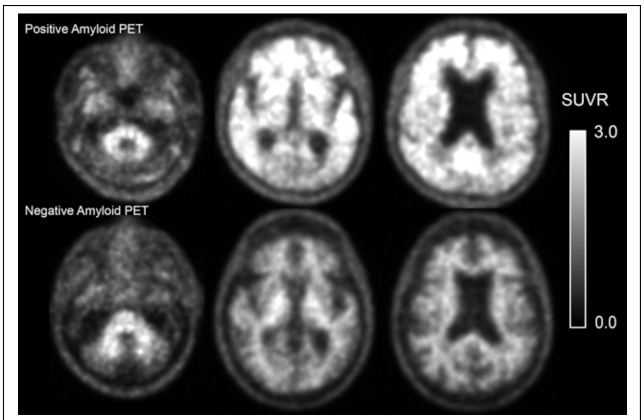

FIGURE 1. Amyloid PET. (Top row) Positive amyloid PET scan with loss of gray–white differentiation and areas of abnormally increased cortical uptake in multiple regions of cerebral hemispheres. This is compatible with presence of moderate to frequent amyloid-β neuritic plaques. (Bottom row) In contrast, negative amyloid PET scan has distinct gray–white contrast in all lobes, with distinctly visible branching white matter tracts. SUVR = SUV ratio.

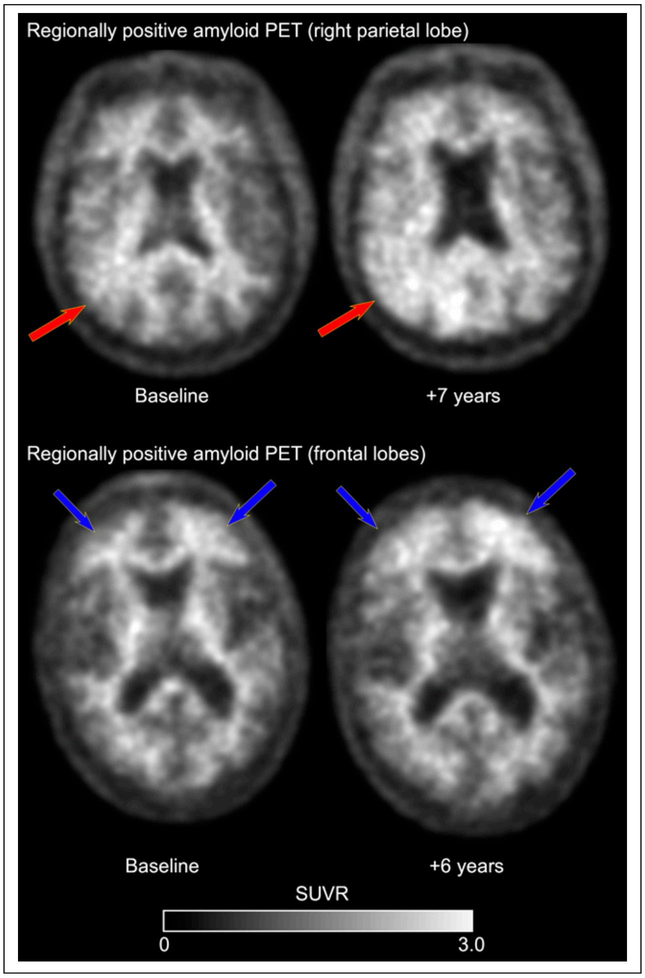

FIGURE 2. Regional positive amyloid PET: baseline and follow-up ^{11}C-PiB PET examinations. (Top row) Right parietal regionally positive examination with loss of gray–white contrast in right parietal lobe. Regional uptake progressed on follow-up in 7 y (arrows) and correlated to amyloid-β neuritic plaques at autopsy. Cerebrospinal fluid markers for amyloid were negative. (Bottom row) Bilateral frontal regionally positive examination with loss of gray–white contrast in left greater than right frontal lobes (arrows). Uptake progressed over 6 y and correlated with frontal amyloid-β neuritic plaques at autopsy. Cerebrospinal fluid markers for amyloid became positive in second case 7 y after baseline PET.

hemispheres for the integrity of the gray–white contrast (Fig. 2). Amyloid PET interpretation can also be challenging in the setting of brain parenchymal volume loss, a common scenario. Enlargement of the cerebrospinal fluid spaces due to volume loss may mimic a normal branching white matter pattern when the PET images are reviewed alone (Supplemental Fig. 1; supplemental materials are available at http://jnm.snmjournals.org). Use of multiplanar reconstructions and fusion with anatomic images can be most helpful for clarification of the outer borders of the cortex. Familiarity with the major white matter tracts can also be helpful, as the association tracts within a cerebral hemisphere should be clearly visible as distinct radiotracer-avid structures (Fig. 1). Other potential pitfalls that may result in an inaccurate interpretation can be technical in nature. A low-count study can reduce gray–white matter contrast, resulting in an inaccurate categorization of a normal scan as positive. When one is systematically reviewing the images, starting with the cerebellum may provide a reliable internal control for the degree of gray–white contrast to expect in the cerebral hemispheres. Increased image noise may be conspicuous in the extracranial soft tissue, an additional indicator of a low-count study. Increased uptake in an extracranial structure, such as the parotid glands, scalp, or even an osseous or intracranial mass, can impact automated windowing and leveling of the study, leading to an inaccurate interpretation. To correct the windowing and leveling of the examination, the abnormally radiotracer-avid structure can be omitted from a selected representative region of the brain that includes cerebral gray and white matter. Some intracranial masses such as meningiomas are known to bind to some amyloid radiotracers, and it is important to avoid mistaking such lesions for radiotracer-avid cortex (Supplemental Fig. 2) (*26*). Anatomic fusion images or comparison MRI examinations may be helpful for confirming the presence of a mass lesion and diagnosing such lesions more definitely.

A limitation of amyloid PET for characterizing AD pathology is that radiotracer binding correlated with both neuritic amyloid-β plaques and diffuse amyloid-β plaques. Diffuse plaques are noncompact deposits that lack neuritic components. Diffuse plaques are commonly found in aged brains and are not specific for AD. A positive amyloid PET study reflective of diffuse plaques may be present in pathologic aging or alternative neurodegenerative diagnoses (Fig. 3) (*27*). Tau PET may potentially provide additional diagnostic certainty. Cases of low amyloid-β plaque burden may be undetectable with amyloid PET, an additional limitation of the imaging modality (*27,28*). Follow-up scans may be useful for detecting progressive amyloid accumulation. Amyloid-β accumulation detected on amyloid PET has been observed with other neurodegenerative processes such as dementia with Lewy bodies, atypical AD, and frontotemporal lobar degeneration, and in isolation, a positive amyloid PET study should not be viewed as sufficient for a diagnosis of AD (*29,30*). Nevertheless, a negative amyloid PET study is able to reliably exclude AD—clinically valuable information in deciding whether to pursue antiamyloid therapy or whether to consider alternative diagnoses.

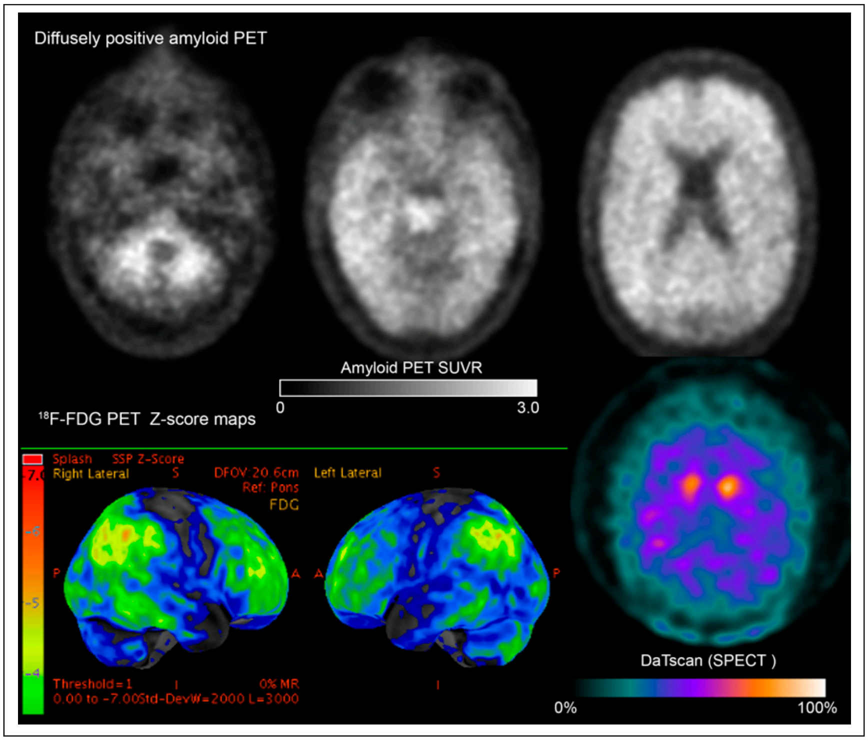

FIGURE 3. Pitfall of diffusely positive amyloid PET in dementia with Lewy bodies. (Top row) ^{11}C-PiB PET is positive and shows diffuse loss of gray–white contrast in both cerebral hemispheres. (Bottom row) ^{18}F-FDG PET *z* score map (left and center) in same person shows hypometabolism in occipital lobes, atypical region for AD, in pattern suggestive of dementia with Lewy bodies. ^{123}I-ioflupane SPECT (DaTscan; GE Healthcare) is abnormal (right), further supporting diagnosis of dementia with Lewy bodies, which was ultimately confirmed at autopsy. In non-Alzheimer neurodegenerative pathology, presence of diffuse plaques without neuritic components may still be associated with abnormal amyloid PET. SUVR = SUV ratio.

TAU PET

The spatial distribution of pathologic tau hyperphosphorylation and neurofibrillary tangle deposition corresponds to AD pathology, as characterized in Braak neurofibrillary tangle staging as a measure of abnormal tau at autopsy. Antemortem evaluation of pathologic tau distribution can be performed with PET. ^{18}F-flortaucipir (AV-1451) is the only FDA-approved radiopharmaceutical for tau PET and has been found to closely follow neurofibrillary tangle Braak staging for AD (Table 4) (*31,32*).

Per the FDA package insert, ^{18}F-flortaucipir is indicated to assess tau burden in cognitively impaired adults being evaluated for AD. The scan should be interpreted without consideration of collateral information such as clinical data or other biomarkers, which may bias the interpretation. At present, tau PET is not indicated for evaluating non-AD tauopathies or chronic traumatic encephalopathy (*32,33*).

^{18}F-flortaucipir binds with high affinity to paired helical filament tau, and abnormal radiotracer binding in the neocortex above background is the basis for identifying a positive tau PET scan (Fig. 4) (*34*). A threshold level of background uptake is set at 1.65-fold the average cerebellar uptake, and the manufacturer-specified display

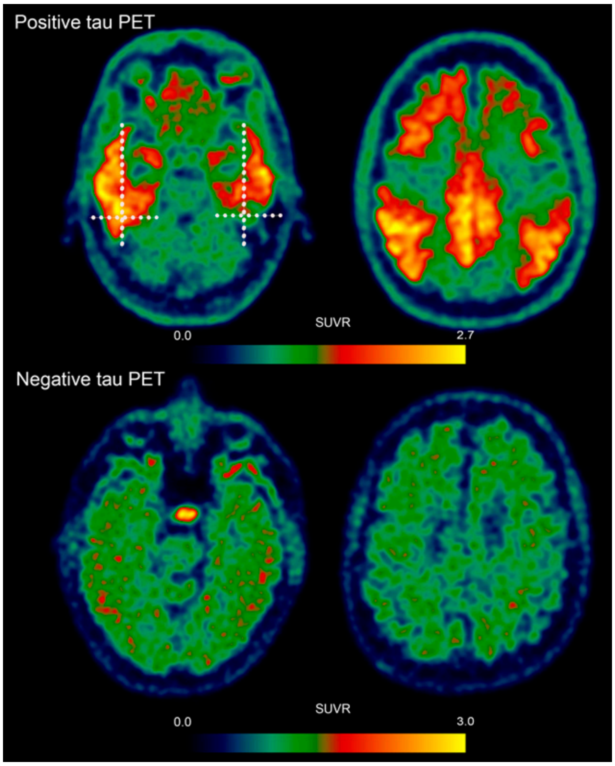

FIGURE 4. Tau PET with ^{18}F-flortaucipir. (Top row) Positive tau PET with areas of abnormally increased (red and orange color overlay) uptake in lateral temporal, frontal, and parietal lobes, including precuneus and posterior cingulate. Temporal lobes are divided into quadrants (dotted lines). Only uptake in posterolateral quadrant of temporal lobe should be used to consider ^{18}F-flortaucipir PET scan positive using visual interpretation. (Bottom row) Negative tau PET with no abnormally increased regions of uptake in cerebral hemispheres. SUVR = SUV ratio.

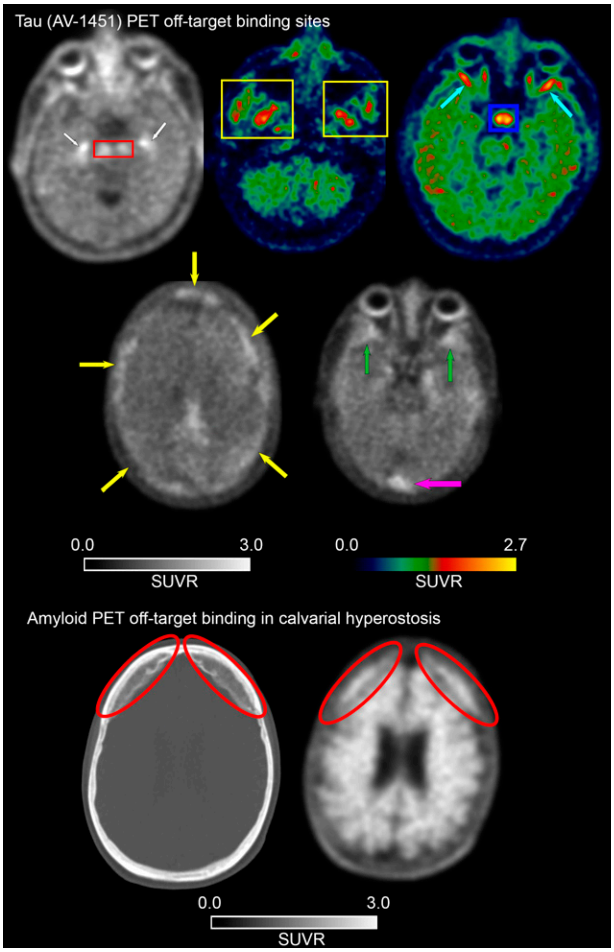

FIGURE 5. Off-target binding on tau and amyloid PET. (Top 2 rows) ^{18}F-flortaucipir PET shows off-target uptake in substantia nigra (red rectangle), choroid plexus (white arrows), muscles of mastication (yellow rectangles), extraocular muscles (cyan arrows), and multiple osseous structure including calvarium (yellow arrows), occiput (pink arrow), and sphenoid bones (green arrows). (Bottom row) Off-target osseous uptake can also be seen on amyloid PET (^{18}F-florbetapir PET/CT) showing avid region of hyperostosis frontalis interna (ellipses), which in some cases could mimic cortical uptake without anatomic correlation. SUVR = SUV ratio.

guidelines for ^{18}F-flortaucipir are devised to set the color scale to show a transition above background level uptake. Sequentially, neocortical uptake should be assessed in each lobe: temporal, occipital, parietal, and frontal. The temporal lobe should be subdivided into quadrants (Fig. 4) including anterolateral, anterior mesial, posterolateral, and posterior mesial temporal. Only the posterolateral temporal quadrant can contribute to classification of a positive tau PET scan. Uptake in the anterior and medial temporal lobe does not meet visual interpretation criteria for a positive tau PET scan. Abnormal uptake in the parietal lobe/precuneus or in the occipital lobes may also qualify a scan as positive for widely distributed tau pathology. Abnormal frontal uptake may or may not be identified in positive scans. Negative scans may have ^{18}F-flortaucipir uptake in the medial or anterolateral temporal lobes, frontal lobes, or deep gray nuclei and white matter (*32,34*).

As with amyloid PET radiotracers, volume loss can be a pitfall, rendering distinction of neocortical binding from white matter uptake difficult. Careful correlation with anatomic images can be useful in the setting of parenchymal volume loss. Small noncontiguous foci of uptake should be interpreted with caution, particularly in scans with increased noise, as these can lead to a false-positive assessment (*35*).

Off-target binding of ^{18}F-flortaucipir is a limitation (Fig. 5) and can involve structures such as the brain stem nuclei and substantia nigra, striatum, choroid plexus, leptomeninges, and blood vessels (*36*). Possible mechanisms have been suggested for off-target binding, such as radiotracer affinity for monoamine oxidase A and B, pigmented compounds such as neuromelanin, and mineralized structures (*32,36*). ^{18}F-flortaucipir binding has also been reported within meningiomas (Supplemental Fig. 2) (*37*). Binding to the leptomeningeal structures could be mistaken for cortical uptake, a pitfall that may be avoided with careful attention to coregistered anatomic images. Off-target binding may potentially be ameliorated with next-generation tau radiotracers (*36*).

^{18}F-flortaucipir uptake correlates strongly with the 3R + 4R isoform of tau associated with AD but is not strongly associated with preferential 3R or 4R isoforms of tau, a limitation of the radiotracer's ability to assess other non-AD tauopathies in cases of Pick disease (3R predominant), corticobasal degeneration (4R predominant), or progressive supranuclear palsy (4R predominant). Weak binding to TDP-43 (transactive response DNA binding protein of 43 kDa) may confound diagnosis in cases of frontotemporal lobar degeneration TDP. Although tau PET is an important biomarker

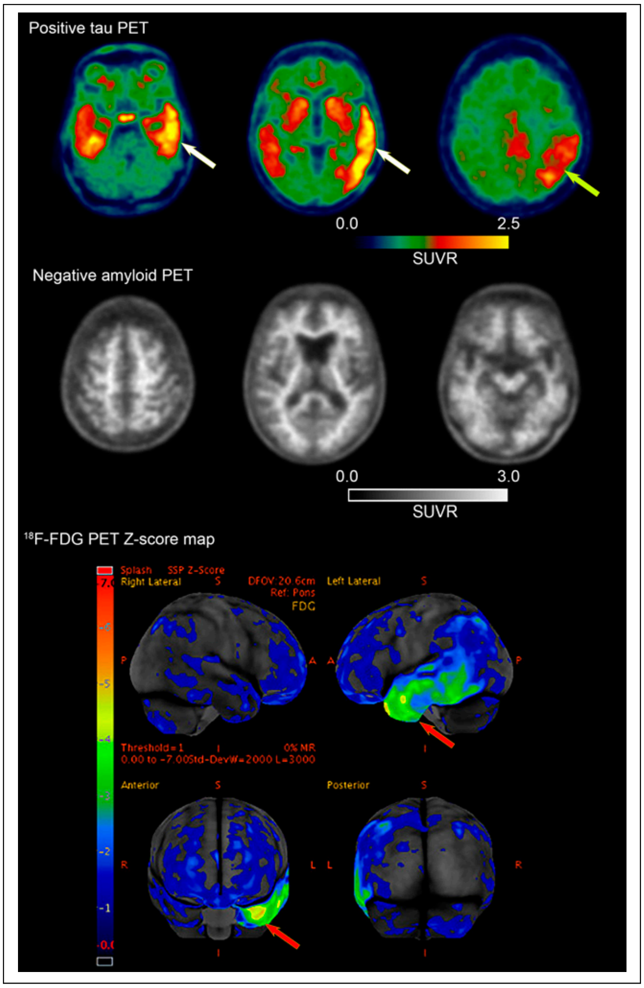

FIGURE 6. Positive tau PET in semantic dementia. (Top row) Multiple PET examinations from patient with semantic dementia, commonly with underlying TDP-43 proteinopathy. ^{18}F-flortaucipir PET was positive, more prominently in left than right temporal lobes (white arrows) and left parietal lobe (yellow arrow). (Second row) ^{11}C-PiB PET was negative, with preserved gray–white contrast indicating lack of moderate or frequent amyloid-β neuritic plaques. (Third and fourth rows) ^{18}F-FDG PET *z* score maps demonstrated regions of hypometabolism correlating with tau PET, worst in left anterior temporal lobe (arrows). Pattern of hypometabolism is characteristic of semantic dementia. Although tau PET was positive, which can be seen with AD, alternative neurodegenerative entities can also result in abnormal tau PET. In this case, negative amyloid PET and pattern of ^{18}F-FDG hypometabolism suggest semantic dementia. SUVR = SUV ratio.

for AD, positive uptake on tau PET can be seen in alternative neurodegenerative conditions such as semantic dementia (Fig. 6) and prion protein defects (Supplemental Fig. 3) (*27,28*).

A significant limitation of ^{18}F-flortaucipir PET in evaluation of AD is poor detection of early tau deposition. According to the FDA package insert instruction for ^{18}F-flortaucipir PET, the regions of early tau deposition corresponding to early Braak stages are to be excluded from visual interpretation (Fig. 4). In general, pathologic tau neurofibrillary tangle accumulation occurs earliest in the mesial temporal structures such as the entorhinal cortex, corresponding with early Braak stage distribution (*38*). Specificity for diagnosing AD on the basis of medial temporal involvement alone may be limited, as this can occur in cognitively unimpaired patients. Tau uptake in the entorhinal cortex, hippocampal formations, parahippocampal gyrus, and middle temporal lobe gyrus strongly correlates with poor memory performance, even in cognitively unimpaired individuals (*39*). One factor limiting accurate assessment of early tau on PET is the detection of low levels of uptake above background noise. Technical developments and innovative image processing techniques may help to improve early tau detection, such as the use of the overlap index in sequential scans (*40*). Future updates in Alzheimer diagnostic criteria may incorporate distinct categories of positive tau PET, distinguishing categories of isolated medial temporal uptake and moderate or high neocortical uptake (*11*). At present, these distinctions are not made in the clinical visual interpretation of tau PET (*32*).

Tau PET in cognitively unimpaired individuals has demonstrated uptake in regions that would correspond to early Braak stage involvement but also in extratemporal locations corresponding to more advanced Braak stages (*38*). The variable distribution of tau pathology in both cognitively unimpaired and cognitively impaired individuals underscores the need for placing a positive tau PET scan within a greater clinical context to support a diagnosis of AD.

DOPAMINERGIC PET

Dopaminergic PET is indicated for the evaluation of parkinsonian syndromes in adults (Table 5) (*41*). Parkinsonian syndromes result from loss of the dopaminergic neurons projecting from the substantia nigra pars compacta to the striatum and presents as a movement disorder characterized by bradykinesia, rigidity, tremor, or postural instability. Typical parkinsonian syndrome (idiopathic Parkinson disease) is the most common parkinsonian syndrome (*13,42*). Other distinct neurodegenerative entities that present as parkinsonian syndromes include dementia with Lewy bodies, progressive supranuclear palsy, multisystem atrophy, and corticobasal degeneration and are collectively termed atypical parkinsonian syndromes (*43*). Typical parkinsonian syndrome is a clinical diagnosis relying of the presence of bradykinesia and either rigidity or rest tremor, as well as other supportive criteria and absence of findings suggesting an alternative diagnosis. Response to dopaminergic therapy is an important supportive criterion for typical parkinsonian syndrome, and poor response is suggestive of an atypical parkinsonian syndrome (*44*).

^{18}F-DOPA is a molecular precursor of the dopamine neurotransmitter, and physiologic uptake is expected in viable presynaptic dopaminergic neurons (*45*). One hour before intravenous radiotracer injection, 150 mg of oral carbidopa should be administered to inhibit peripheral decarboxylation of ^{18}F-FODA and augment brain radiotracer availability. Multiple drug classes used in treated

TABLE 5
^{18}F-DOPA Properties

Administered activity (MBq)	Uptake time (min)	PET scan duration	Positive scan criteria
185	80	20	Loss of caudate or putamen uptake above background

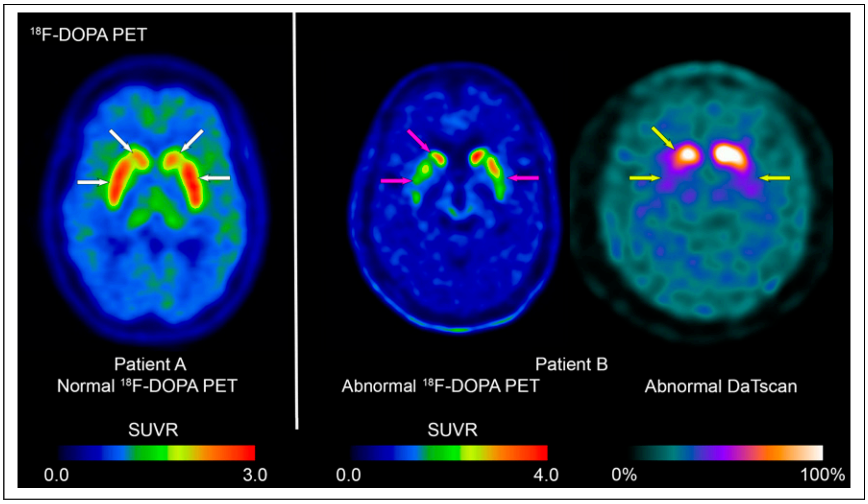

FIGURE 7. Dopaminergic PET. (Left) Normal ^{18}F-DOPA PET examination with expected uptake in caudate and putamen bilaterally (arrows). (Center) Abnormal ^{18}F-DOPA PET examination in 43-y-old woman with onset of Parkinson disease at early age. Abnormal examination shows diminished uptake in bilateral putamina, asymmetrically worse on patient's right, and subtle decreased uptake in patient's right caudate (arrows). (Right) In same patient, ^{123}I-ioflupane SPECT (DaTscan; GE Healthcare) was also abnormal, with decreased basal ganglia uptake (arrows) causing loss of expected comma-shaped region of uptake, asymmetrically worse on patient's right. SUVR = SUV ratio.

parkinsonian syndromes should be discontinued 12 h before radiotracer injection, including dopamine agonists, reuptake inhibitors, releasing agents, catechol-*O*-methyltransferase inhibitors, and monoamine oxidase inhibitors. After ^{18}F-DOPA injection and uptake, a 3-dimensional PET acquisition is recommended. Axial images should be reconstructed along the anterior–posterior commissure line. Images are to be interpreted on the basis of visual inspection, without collateral clinical information used to influence the classification as normal or abnormal (*41*).

A normal (negative) scan should demonstrate radiotracer-avid basal ganglia structures including the caudate head and putamen (Fig. 7), together forming a crescent shape. A positive (abnormal) scan may have asymmetric or symmetric reduction of uptake in the putamen, resulting in either diminished intensity of uptake or a truncated region of uptake in the putamen. Uptake may also be reduced in the caudate nuclei in a positive scan.

A positive scan may indicate a typical or atypical parkinsonian syndrome by detecting loss of striatal dopaminergic neurons in Parkinson disease, progressive supranuclear palsy, corticobasal degeneration, and multiple-system atrophy. Dopaminergic PET may also be useful in diagnosing dementia with Lewy bodies (*46*). These different entities cannot be distinguished on the basis of dopaminergic PET. Conditions resulting in a negative scan may include essential tremor or other causes of parkinsonian syndromes including pharmacologic, psychogenic, or vascular etiologies (*15*). In vascular parkinsonism, correlation with anatomic imaging may help avoid an interpretation pitfall. A basal ganglia infarct may explain the patient's symptoms and could result in an abnormal truncated appearance on dopaminergic PET.

^{18}F-DOPA PET has been reported to have a diagnostic performance similar to that of ^{123}I-ioflupane SPECT/CT; however, some discrepancies have been reported, suggesting that more cases are positive with ^{123}I-ioflupane SPECT (*47–49*). In the setting of dopaminergic neuron loss, upregulation of dopamine synthesis in the residual neurons could preserve uptake of ^{18}F-DOPA relative to ^{123}I-ioflupane. Advantages of ^{18}F-DOPA PET include improved spatial resolution and a shorter uptake time of 1.5 h, compared with 3–6 h for ^{123}I ioflupane SPECT (*41,50*). At present, ^{123}I-ioflupane SPECT is more widely available and reimbursed.

Multiple investigational agents can image the dopaminergic and monoaminergic systems, including postsynaptic dopamine receptor ligands and presynaptic targets such as the dopamine active transporter. ^{18}F-DOPA and ^{123}I-ioflupane are the radiopharmaceuticals used clinically in the United States, with ^{123}I-ioflupane being more frequently used (*51,52*).

In addition to parkinsonian syndromes, dopaminergic PET has been investigated for use in evaluation of schizophrenia, psychosis, and glioma but does not have current FDA regulatory approval for these indications (*53,54*).

CONCLUSION

Multiradiopharmaceutical assessment with amyloid, tau, and ^{18}F-FDG PET provides a relatively comprehensive characterization of the different components of Alzheimer pathophysiology. Amyloid and tau PET contribute a greater level of detail and diagnostic certainty in characterizing AD pathophysiology, which may be critical, particularly when evaluating patients for antiamyloid therapies. Furthermore, amyloid PET confirms the therapeutic target for these therapies.

The multiple PET radiopharmaceuticals discussed in this review can yield a robust characterization of neuropathologic processes, but inherent limitations to the multiple-biomarker approach remain. Challenges remain in detecting early abnormal amyloid and tau on PET. At present, no clinically available radiopharmaceuticals are available for evaluation of some important proteinopathies, including TDP-43 and certain isoforms of tau. Furthermore, reliance on multiple-radiopharmaceutical PET examinations come with increased societal health care costs, increased direct costs to patients, and practical challenges of performing multiple imaging studies. For these reasons, the ability of ^{18}F-FDG PET to distinguish a variety of neurodegenerative patterns and functional information with a single examination is one advantage over the amyloid, tau, and dopaminergic PET examinations discussed in this review.

Familiarity with the visual interpretation methods and protocols for amyloid and tau PET is essential for accurate categorization of a positive or negative scan. For amyloid PET, careful correlation with anatomic imaging may help avoid pitfalls in interpretation such as the common scenario of an abnormal amyloid PET scan with advanced brain parenchymal volume loss, which can mimic normal white matter uptake. For tau PET, knowledge of which regions may have off-target radiotracer binding and which brain parenchymal regions should be excluded from visual interpretation is important for accurate interpretation.

Dopaminergic PET characterizes parkinsonian syndromes but may be abnormal in a variety of parkinsonian syndrome etiologies. Awareness that multiple medications may interfere with uptake is important for avoid a misleading result.

The variety of brain PET radiopharmaceuticals increasingly seen in clinical practice is an indicator of the complexity of dementia. Advances in the in vivo characterization of dementia with PET will likely continue to augment our understanding of the underlying pathophysiology and facilitate evaluation of innovative therapies.

REFERENCES

1. *The Global Dementia Observatory Reference Guide.* World Health Organization; 2018.
2. Hall B, Mak E, Cervenka S, Aigbirhio FI, Rowe JB, O'Brien JT. In vivo tau PET imaging in dementia: pathophysiology, radiotracer quantification, and a systematic review of clinical findings. *Ageing Res Rev.* 2017;36:50–63.
3. Minoshima S, Cross D, Thientunyakit T, Foster NL, Drzezga A. ^{18}F-FDG PET imaging in neurodegenerative dementing disorders: insights into subtype classification, emerging disease categories, and mixed dementia with copathologies. *J Nucl Med.* 2022;63(supp 1):2S–12S.
4. Burkett BJ, Babcock JC, Lowe VJ, Graff-Radford J, Subramaniam RM, Johnson DR. PET imaging of dementia: update 2022. *Clin Nucl Med.* 2022;47:763–773.
5. Mena AM, Strafella AP. Imaging pathological tau in atypical parkinsonisms: a review. *Clin Park Relat Disord.* 2022;7:100155.
6. Jack CR, Bennett DA, Blennow K, et al. NIA-AA research framework: toward a biological definition of Alzheimer's disease. *Alzheimers Dement.* 2018;14:535–562.
7. Kantarci K. 2021 marks a new era for Alzheimer's therapeutics. *Lancet Neurol.* 2022;21:3–4.
8. Jack CR Jr, Bennett DA, Blennow K, et al. A/T/N: an unbiased descriptive classification scheme for Alzheimer disease biomarkers. *Neurology.* 2016;87:539–547.
9. Mukku SSR, Sivakumar PT, Nagaraj C, Mangalore S, Harbishettar V, Varghese M. Clinical utility of ^{18}F-FDG-PET/MRI brain in dementia: preliminary experience from a geriatric clinic in South India. *Asian J Psychiatr.* 2019;44:99–105.
10. Pagani M, Nobili F, Morbelli S, et al. Early identification of MCI converting to AD: a FDG PET study. *Eur J Nucl Med Mol Imaging.* 2017;44:2042–2052.
11. Revised Criteria for Diagnosis and Staging of Alzheimer's Disease: Alzheimer's Association Workgroup. Alzheimer's Association website. https://aaic.alz.org/diagnostic-criteria.asp#drafts. Accessed April 8, 2024.
12. Oldan JD, Jewells VL, Pieper B, Wong TZ. Complete evaluation of dementia: PET and MRI Correlation and diagnosis for the neuroradiologist. *AJNR.* 2021;42:998–1007.
13. Broski SM, Hunt CH, Johnson GB, Morreale RF, Lowe VJ, Peller PJ. Structural and functional imaging in parkinsonian syndromes. *Radiographics.* 2014;34:1273–1292.
14. Mhyre TR, Boyd JT, Hamill RW, Maguire-Zeiss KA. Parkinson's disease. *Subcell Biochem.* 2012;65:389–455.
15. Ibrahim N, Kusmirek J, Struck AF, et al. The sensitivity and specificity of F-DOPA PET in a movement disorder clinic. *Am J Nucl Med Mol Imaging.* 2016;6:102–109.
16. Johnson KA, Minoshima S, Bohnen NI, et al. Appropriate use criteria for amyloid PET: a report of the Amyloid Imaging Task Force, the Society of Nuclear Medicine and Molecular Imaging, and the Alzheimer's Association. *J Nucl Med.* 2013;54:476–490.
17. Minoshima S, Drzezga AE, Barthel H, et al. SNMMI procedure standard/EANM practice guideline for amyloid PET imaging of the brain 1.0. *J Nucl Med.* 2016;57:1316–1322.
18. Ramanan VK, Day GS. Anti-amyloid therapies for Alzheimer disease: finally, good news for patients. *Mol Neurodegener.* 2023;18:42.
19. Budd Haeberlein S, Aisen PS, Barkhof F, et al. Two randomized phase 3 studies of aducanumab in early Alzheimer's disease. *J Prev Alzheimers Dis.* 2022;9:197–210.
20. McDade E, Cummings JL, Dhadda S, et al. Lecanemab in patients with early Alzheimer's disease: detailed results on biomarker, cognitive, and clinical effects from the randomized and open-label extension of the phase 2 proof-of-concept study. *Alzheimers Res Ther.* 2022;14:191.
21. Swanson CJ, Zhang Y, Dhadda S, et al. A randomized, double-blind, phase 2b proof-of-concept clinical trial in early Alzheimer's disease with lecanemab, an anti-Aβ protofibril antibody. *Alzheimers Res Ther.* 2021;13:80.
22. Klunk WE, Engler H, Nordberg A, et al. Imaging brain amyloid in Alzheimer's disease with Pittsburgh compound-B. *Ann Neurol.* 2004;55:306–319.
23. Vizamyl^{TM} flutemetamol F 18 injection. U.S. Food and Drug Administration website. https://www.accessdata.fda.gov/drugsatfda_docs/label/2017/203137s008lbl.pdf. Revised February 2017. Accessed April 8, 2024.
24. Amyvid (florbetapir F 18 injection) for intravenous use. U.S. Food and Drug Administration website. https://www.accessdata.fda.gov/drugsatfda_docs/label/2012/202008s000lbl.pdf. Revised April 2012. Accessed April 8, 2024.
25. NEURACEQ (florbetaben F 18 injection), for intravenous use. U.S. Food and Drug Administration website. https://www.accessdata.fda.gov/drugsatfda_docs/label/2014/204677s000lbl.pdf. Revised March 2014. Accessed April 8, 2024.
26. Johnson DR, Hunt CH, Nathan MA, et al. Pittsburgh compound B (PiB) PET imaging of meningioma and other intracranial tumors. *J Neurooncol.* 2018;136:373–378.
27. Lowe VJ, Lundt ES, Albertson SM, et al. Neuroimaging correlates with neuropathologic schemes in neurodegenerative disease. *Alzheimers Dement.* 2019;15:927–939.
28. Lowe VJ, Lundt ES, Albertson SM, et al. Tau-positron emission tomography correlates with neuropathology findings. *Alzheimers Dement.* 2020;16:561–571.
29. Nedelska Z, Schwarz CG, Lesnick TG, et al. Association of longitudinal β-amyloid accumulation determined by positron emission tomography with clinical and cognitive decline in adults with probable Lewy body dementia. *JAMA Netw Open.* 2019;2:e1916439.
30. Whitwell JL, Tosakulwong N, Weigand SD, et al. Longitudinal amyloid-β PET in atypical Alzheimer's disease and frontotemporal lobar degeneration. *J Alzheimers Dis.* 2020;74:377–389.
31. Fleisher AS, Pontecorvo MJ, Devous MD Sr, et al. Positron emission tomography imaging with [^{18}F]flortaucipir and postmortem assessment of Alzheimer disease neuropathologic changes. *JAMA Neurol.* 2020;77:829–839.
32. TAUVID^{TM} (flortaucipir F 18 injection), for intravenous use. U.S. Food and Drug Administration website. https://www.accessdata.fda.gov/drugsatfda_docs/label/2020/212123s000lbl.pdf. Revised May 2020. Accessed April 8, 2024.
33. Tian M, Civelek AC, Carrio I, et al. International consensus on the use of tau PET imaging agent ^{18}F-flortaucipir in Alzheimer's disease. *Eur J Nucl Med Mol Imaging.* 2022;49:895–904.
34. Groot C, Villeneuve S, Smith R, Hansson O, Ossenkoppele R. Tau PET imaging in neurodegenerative disorders. *J Nucl Med.* 2022;63(suppl 1):20S–26S.
35. Chen CD, Ponisio MR, Lang JA, et al. Comparing tau PET visual interpretation with tau PET quantification, cerebrospinal fluid biomarkers, and longitudinal clinical assessment. *J Alzheimers Dis.* 2023;93:765–777.
36. Lowe VJ, Curran G, Fang P, et al. An autoradiographic evaluation of AV-1451 tau PET in dementia. *Acta Neuropathol Commun.* 2016;4:58.
37. Bruinsma TJ, Johnson DR, Fang P, et al. Uptake of AV-1451 in meningiomas. *Ann Nucl Med.* 2017;31:736–743.
38. Lowe VJ, Wiste HJ, Senjem ML, et al. Widespread brain tau and its association with ageing, Braak stage and Alzheimer's dementia. *Brain.* 2018;141:271–287.
39. Lowe VJ, Bruinsma TJ, Wiste HJ, et al. Cross-sectional associations of tau-PET signal with cognition in cognitively unimpaired adults. *Neurology.* 2019;93:e29–e39.
40. Lee J, Burkett BJ, Min HK, et al. Deep learning-based brain age prediction in normal aging and dementia. *Nat Aging.* 2022;2:412–424.
41. FLUORODOPA F 18 injection, for intravenous use. U.S. Food and Drug Administration website. https://www.accessdata.fda.gov/drugsatfda_docs/label/2019/200655s000lbl.pdf. Revised October 2019. Accessed April 8, 2024.
42. Postuma RB, Berg D, Stern M, et al. MDS clinical diagnostic criteria for Parkinson's disease. *Mov Disord.* 2015;30:1591–1601.
43. Levin J, Kurz A, Arzberger T, Giese A, Höglinger GU. The differential diagnosis and treatment of atypical parkinsonism. *Dtsch Arztebl Int.* 2016;113:61–69.
44. Goetz CG, Tilley BC, Shaftman SR, et al. Movement Disorder Society-sponsored revision of the Unified Parkinson's Disease Rating Scale (MDS-UPDRS): scale presentation and clinimetric testing results. *Mov Disord.* 2008;23:2129–2170.
45. Pretze M, Wängler C, Wängler B. 6-[^{18}F]fluoro-L-DOPA: a well-established neurotracer with expanding application spectrum and strongly improved radiosyntheses. *BioMed Res Int.* 2014;2014:674063.
46. Hu XS, Okamura N, Arai H, et al. ^{18}F-fluorodopa PET study of striatal dopamine uptake in the diagnosis of dementia with Lewy bodies. *Neurology.* 2000;55:1575–1577.
47. Eshuis SA, Maguire RP, Leenders KL, Jonkman S, Jager PL. Comparison of FP-CIT SPECT with F-DOPA PET in patients with de novo and advanced Parkinson's disease. *Eur J Nucl Med Mol Imaging.* 2006;33:200–209.
48. Ishikawa T, Dhawan V, Kazumata K, et al. Comparative nigrostriatal dopaminergic imaging with iodine-123-beta CIT-FP/SPECT and fluorine-18-FDOPA/PET. *J Nucl Med.* 1996;37:1760–1765.
49. Wallert E, Letort E, van der Zant F, et al. Comparison of [^{18}F]-FDOPA PET and [^{123}I]-FP-CIT SPECT acquired in clinical practice for assessing nigrostriatal degeneration in patients with a clinically uncertain parkinsonian syndrome. *EJNMMI Res.* 2022;12:68.
50. Banks KP, Peacock JG, Clemenshaw MN, Kuo PH. Optimizing the diagnosis of parkinsonian syndromes with ^{123}I-ioflupane brain SPECT. *AJR.* 2019;213:243–253.
51. Kanthan M, Cumming P, Hooker JM, Vasdev N. Classics in neuroimaging: imaging the dopaminergic pathway with PET. *ACS Chem Neurosci.* 2017;8:1817–1819.
52. Post MR, Sulzer D. The chemical tools for imaging dopamine release. *Cell Chem Biol.* 2021;28:748–764.
53. Veronese M, Santangelo B, Jauhar S, et al. A potential biomarker for treatment stratification in psychosis: evaluation of an [^{18}F] FDOPA PET imaging approach. *Neuropsychopharmacology.* 2021;46:1122–1132.
54. Pafundi DH, Laack NN, Youland RS, et al. Biopsy validation of ^{18}F-DOPA PET and biodistribution in gliomas for neurosurgical planning and radiotherapy target delineation: results of a prospective pilot study. *Neuro Oncol.* 2013;15:1058–1067.